NASA/TM-2009-215771

Design of Quiet Rotorcraft Approach
Trajectories

Sharon L. Padula, Casey L. Burley, D. Douglas Boyd, Jr., and Michael A. Marcolini
Langley Research Center, Hampton, Virginia

June 2009

NASA STI Program . . . in Profile

Since its founding, NASA has been dedicated to the advancement of aeronautics and space science. The NASA scientific and technical information (STI) program plays a key part in helping NASA maintain this important role.

The NASA STI program operates under the auspices of the Agency Chief Information Officer. It collects, organizes, provides for archiving, and disseminates NASA's STI. The NASA STI program provides access to the NASA Aeronautics and Space Database and its public interface, the NASA Technical Report Server, thus providing one of the largest collections of aeronautical and space science STI in the world. Results are published in both non-NASA channels and by NASA in the NASA STI Report Series, which includes the following report types:

- TECHNICAL PUBLICATION. Reports of completed research or a major significant phase of research that present the results of NASA programs and include extensive data or theoretical analysis. Includes compilations of significant scientific and technical data and information deemed to be of continuing reference value. NASA counterpart of peer-reviewed formal professional papers, but having less stringent limitations on manuscript length and extent of graphic presentations.

- TECHNICAL MEMORANDUM. Scientific and technical findings that are preliminary or of specialized interest, e.g., quick release reports, working papers, and bibliographies that contain minimal annotation. Does not contain extensive analysis.

- CONTRACTOR REPORT. Scientific and technical findings by NASA-sponsored contractors and grantees.

- CONFERENCE PUBLICATION. Collected papers from scientific and technical conferences, symposia, seminars, or other meetings sponsored or co-sponsored by NASA.

- SPECIAL PUBLICATION. Scientific, technical, or historical information from NASA programs, projects, and missions, often concerned with subjects having substantial public interest.

- TECHNICAL TRANSLATION. English-language translations of foreign scientific and technical material pertinent to NASA's mission.

Specialized services also include creating custom thesauri, building customized databases, and organizing and publishing research results.

For more information about the NASA STI program, see the following:

- Access the NASA STI program home page at *http://www.sti.nasa.gov*

- E-mail your question via the Internet to *help@sti.nasa.gov*

- Fax your question to the NASA STI Help Desk at 443-757-5803

- Phone the NASA STI Help Desk at 443-757-5802

- Write to:
  NASA STI Help Desk
  NASA Center for AeroSpace Information
  7115 Standard Drive
  Hanover, MD 21076-1320

NASA/TM-2009-215771

Design of Quiet Rotorcraft Approach Trajectories

Sharon L. Padula, Casey L. Burley, D. Douglas Boyd, Jr., and Michael A. Marcolini
Langley Research Center, Hampton, Virginia

June 2009

Abstract

A optimization procedure for identifying quiet rotorcraft approach trajectories is proposed and demonstrated. The procedure employs a multi-objective genetic algorithm in order to reduce noise and create approach paths that will be acceptable to pilots and passengers. The concept is demonstrated by application to two different helicopters. The optimized paths are compared with one another and to a standard 6-deg approach path. The two demonstration cases validate the optimization procedure but highlight the need for improved noise prediction techniques and for additional rotorcraft acoustic data sets.

Introduction

Background

The Subsonic Rotary Wing (SRW) project under the NASA Fundamental Aeronautics Program seeks to develop multidisciplinary design optimization (MDO) tools that enable the design and operation of safe and environmentally compatible rotorcraft. One segment of the SRW project emphasizes vehicle aeroacoustics and noise propagation tools. For example, the present study develops trajectory optimization techniques for reducing community noise near helipads. The present study builds upon past theoretical and experimental research sponsored by industry, government, and academia.

The rotorcraft industry sponsors MDO research that involves topics such as structural dynamics, aerodynamics, noise mechanisms, noise propagation, and modified takeoff and landing procedures. For example, Orr and Narducci provide a summary of current MDO research at Boeing Helicopters (ref. 1). In addition to industry internal research and development efforts, a consortium of industry partners sponsors noise measurement activities and supports the Helicopter Association International (HAI) Fly Neighborly Program to educate pilots about low-noise operating procedures (refs. 2 and 3).

The U.S. Government military and civilian laboratories perform fundamental research in noise prediction methods and noise reduction technologies, and sponsor rotorcraft flight and wind-tunnel testing (refs. 4 and 5). This fundamental research has produced a number of software tools, such as the Rotorcraft Noise Model (RNM) that is described in reference 6. The RNM code uses a database of measured or predicted noise hemispheres as input to predict the noise footprint for a given rotorcraft flight path (see fig. 1). The RNM code can provide a wide variety of noise metrics, such as time histories of overall sound pressure level (OASPL) and sound exposure level (SEL) noise footprints. The calculations can include the effects of uneven terrain, layered atmosphere with attenuation, ground attenuation, and ground reflections.
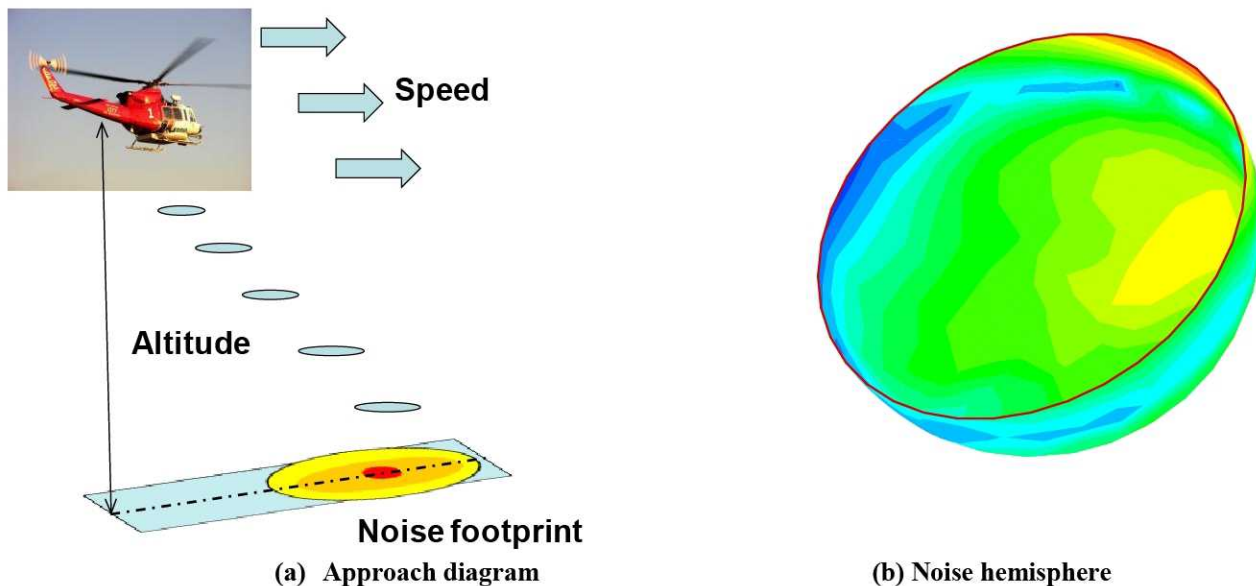
(a) Approach diagram   (b) Noise hemisphere

Figure 1. RNM approach path diagram and representative noise hemisphere.

Scope

The present research uses the RNM code to predict the community noise that is generated by a helicopter; a segmented approach with linearly varying parameters on each segment is assumed. A standard atmosphere is also assumed and ground effects (reflection and attenuation) are included. This research uses the iSight framework[*] (a product of Engineous Software, Inc.) to automate the determination of optimized flight paths. Two different helicopters are considered in this paper, the Bell CH−146 and McDonnell Douglas MD−900. The CH−146 optimization effort uses measured noise hemispheres, and the MD−900 effort uses predicted noise hemispheres. The best approach trajectories that were identified for each helicopter are compared with one another and with a standard approach that uses a 6-deg descent angle. The acceptability of the optimized approach is assessed by comparing it with the guidelines that are discussed in references 2 through 4.

The proposed optimization strategy employs a multi-objective genetic algorithm (MOGA) to simultaneously reduce average community noise and average rate of descent. The iSight framework provides software tools to wrap the RNM code; to define and calculate optimization design variables, objective functions and constraint functions; and to iterate between the RNM and MOGA codes. The MOGA generates a large number of possible approach trajectories and uses an optimization strategy to converge to the best one.

This paper describes the optimization problem, provides sample results, and makes recommendations for future experimental testing and validation of the results. Section 2 discusses the optimization problem, and proposes design variables, objective functions, and constraints for the optimization problem. Section 3 discusses results for the CH−146 helicopter and identifies some issues that are associated with the RNM, the MOGA, and the CH−146 experimental data set. Section 4 discusses results for the MD−900 helicopter and demonstrates an improved version of the MOGA. Section 5 provides concluding remarks and suggestions for future research.

---

[*] The use of trademarks or names of manufacturers in this report is for accurate reporting and does not constitute an official endorsement, either expressed or implied, of such products or manufacturers by the National Aeronautics and Space Administration.

Optimization Strategy

MOGA

Multi-objective genetic algorithms (MOGA) are a popular class of combinatorial optimization methods. MOGA algorithms randomly create a large population of candidate designs and then generate improved designs by merging the best traits of each of the candidate designs. MOGA are not computationally efficient but are easy to apply to a wide variety of optimization problems. MOGA do not calculate gradients; therefore, they can tolerate analysis codes that return no result or an anomalous result for certain values of the design variables. MOGA generate random combinations of design variables; therefore they can converge to one or more excellent solutions that are quite different from the best-known solution. MOGA are especially appropriate to trajectory optimization problems because these problems tend to have a few excellent solutions that differ from one another. Many variants of the MOGA optimization method exist. The MOGA software that is provided by the iSight framework is based on the Nondominated Sorting Genetic Algorithm II that is described in reference 7.

Design Variables

Noise caused by an aircraft flyover is known to depend on vehicle speed and altitude as a function of time (e.g., see ref. 8). The angle between the vehicle and the observer is another important factor. As pictured in figure 1, helicopter source noise on a hemisphere of constant radius is usually louder (i.e., more red) in the right forward quadrant. Thus, finding the quietest approach path requires a tradeoff between landing quickly, approaching steeply, and maintaining an approach angle that exposes the community to the lowest source noise, while still remaining within the safe operating envelope of the vehicle.

Selecting the appropriate design variables to parameterize the approach path is essential. The computational cost of the MOGA increases with the number of design variables. Therefore, the number of design variables must be reduced if possible. In addition, the design variables must be scaled so that all have the same order of magnitude; otherwise, one design variable can dominate the optimization results. Finally, each possible set of design variable values must create a reasonable approach path; otherwise, most of the computer time will be spent evaluating and rejecting poor candidate paths.

Unfortunately, the approach path parametrization that is used by the RNM does not meet the needs of the MOGA. The RNM input describes a flight path in terms of altitude and speed at a set of fixed distances from the helipad. The present research defines the flight path by using 35 linear path segments. This suggests a parameterization with 105 variables (i.e., 35 distances, 35 altitudes, and 35 speeds). The parameterization is unfortunate because of the large number of variables and because the value of speed is two orders of magnitude smaller than the value of distance. Moreover, random changes to any of the 105 variable values will typically produce approach paths with both acceleration and deceleration and with abrupt changes in altitude. This sort of roller coaster approach path is not acceptable to passengers.

An alternate parameterization of the approach path has only 14 design variables and produces a wide variety of acceptable candidate approach paths. The new design variables have small integer values and are used to select the initial altitude, the initial speed, and the percentage of change in speed and descent rate for each of the next 11 approach path segments. The CH−146 optimization effort uses fixed distances for each of the flight path segments. The improved MD−900 optimization effort uses variable distances. In the MD−900 effort, the initial distance is fixed, but the distance at which descent begins and ends varies. In both optimization efforts, the values of integer design variables are converted into the physical distances, altitudes, and speeds by using simple arithmetic equations which are given below. The advantages of this new parameterization are that the integer design variables all have similar magnitudes

and they automatically create flight paths that are smooth and monotonically descending. The calculation of physical units and the creation of the RNM input file are easily accomplished in the iSight framework.

Metrics

Previous studies have compared candidate quiet approach procedures with an approach path that has a constant 6-deg descent , which is herein referred to as a standard approach. Reference 8 demonstrates that the 6-deg approach path that is specified by FAR-36 for rotorcraft certification is not a low-noise approach path for the XV−15 tiltrotor. Reference 9 proposes several quiet approach procedures for the XV−15 and notes that flight along a 6-deg flight path produces increased noise at approach speeds from 60 to 100 knots. References 3 and 4 contain acoustic flight test results for a wide variety of helicopters and both conclude that the 6-deg approach path that is specified for certification is rarely the best choice for day-to-day operations. The present paper extends the research begun in references 3 through 9 and develops an optimization-based strategy for identifying quiet approach paths for any type of rotorcraft.

The success of the optimization process is evaluated by comparing the optimized approach path with the standard 6-deg approach path. For this purpose, the standard approach path is defined as having a level flight segment at an altitude of 1400 ft and a 6-deg descent segment from an altitude of 1400 ft to 300 ft. The vehicle decelerates from 100 to 63 kt along this approach path. The speed and altitude as a function of distance from the helipad are pictured in figure 2. This standard approach is appropriate for both the MD−900 and the CH−146 helicopter and is similar to the decelerating 6-deg approach that is discussed in reference 4.
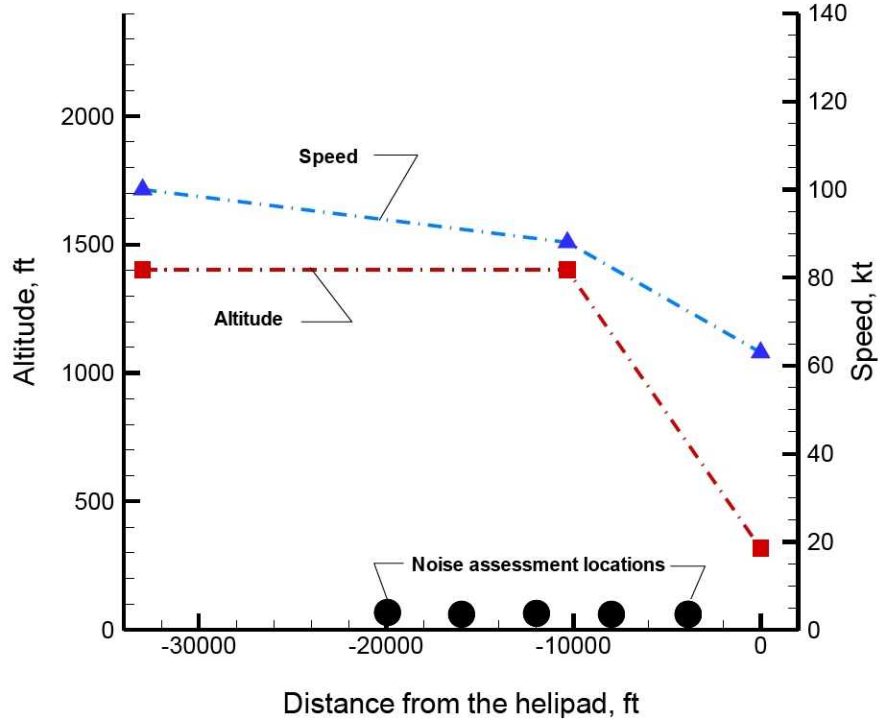

Figure 2. Standard approach path and noise assessment locations defined.

4

The most important objective of the optimization process is to reduce community noise. Normally, this would mean reducing the noise at every location surrounding the helipad (recall the noise footprint in figure 1). However, for the current demonstration, noise is reduced at five locations that are directly under the flight track and located 4000, 8000, 12000, 16000, and 20000 ft from the helipad. These locations are shown as black dots in figure 2.

At each location, the SEL is computed. Reference 10 explains that the SEL is based on the maximum A-weighted sound level with a duration correction for the length of time that the sound level is at or near this maximum value. This measure is sometimes referred to as noise exposure level and can be represented by acronyms or symbols such as SEL, NEL, L_{AX}, or L_S. In this paper, the acronym SELA is used to denote the value of the SEL that is computed by the RNM code. The SELA is deemed appropriate for community noise because annoyance is affected by sound level, sound duration, and source frequency. The average noise reduction is determined by comparing the SELA levels for the optimized approach path with the levels that were estimated for the standard 6-deg approach. Thus, the average change in noise is computed as

$$S_{ave} = \frac{1}{n}\sum_{i=1}^{n} \Delta SELA_i \qquad (1)$$

where $n = 5$ and $\Delta SELA_i$ is the difference at location i between the SELA that is estimated for the current approach path and the SELA that is estimated for the standard approach path. Hence, the goal is to minimize S_{ave} and to obtain negative values for each $\Delta SELA_i$. Experience has shown that reducing noise at several locations under the flight track tends to reduce community noise (e.g., see ref. 8). However, equation (1) can be applied in other ways. The S_{ave} can be calculated with the large number of locations required to create a noise footprint. Alternately, because the area that surrounds the helipad may include both industrial and residential zones, the noise assessment locations could be placed only in the most noise-sensitive areas.

Another important objective of the optimization process is to create an approach path that is acceptable to pilots and passengers. Reference 9 discusses detailed procedures for evaluating handling qualities and pilot acceptance. For this study, a simplified criterion based on the rate of descent as a function of time is used to decide whether a given flight path is likely to be an acceptable choice. The RNM can produce a detailed time history of flight conditions, including interpolated values of speed and flight path angle. At each time step, the following parameters are calculated from the RNM output:

$$v = s * \frac{0.51444}{0.00508} \qquad r_d = v * \sin(\gamma * \pi/180) \qquad R = -r_d/z \qquad (2)$$

Here, s is the speed in kt, v is speed in ft/min, γ is the flight path angle in deg, r_d is the rate of descent in ft/min, z is the altitude in ft, and R is the rate-of-descent ratio. Acceptable values of r_d are roughly –1000 ft/min at 1000 ft of altitude. At lower altitudes, pilots prefer to descend more gradually. A rule of thumb for determining acceptable descent rates is "at an altitude of x ft, the descent rate should not exceed x ft/min" (e.g., see ref. 9). In other words, a rate-of-descent ratio R that is close to unity is desirable.

Special safe landing rules apply when the helicopter is operated at very low altitude and slow speed. The famous dead man's curve defines a set of low-speed flight conditions for which handling qualities degrade and pilot response is too slow to recover from the loss of engine power.

For this study, an acceptable flight path is one where the average rate-of-descent ratio R_{ave} is less than 1.0 and the maximum rate-of-descent ratio R_{max} is less than 2.0. This constraint on R_{max} matches the highest descent rate for the standard 6-deg approach pictured in figure 2. All flight paths, including the standard one, will start at or above an altitude of 1000 ft and end at an altitude of approximately 300 ft. The

landing segment of the flight path from 300 ft to the ground is assumed to be the same for all flight paths. The optimizer has two objective functions: minimize the average change in SELA (S_{ave}) and minimize the average rate of descent ratio (R_{ave}). The first objective addresses community noise, and the second objective addresses passenger safety and comfort. Note that S_{ave} can be an order of magnitude larger than R_{ave} and, thus, will have a bigger influence on the optimized results.

Low-Noise Approach Path

Reference 2 suggests that pilots should choose an approach path (i.e., glide slope) that avoids main rotor blade-vortex interaction (BVI) noise. BVI noise occurs when the rotor blades intersect the tip vortices from previous blade passages as the vehicle descends. Reference 2 suggests that pilots avoid certain combinations of speed (s) and rate of descent (r_d), which are indicated by a white ovoid in figure 3. Reference 2 explains that the best glide slope for each rotorcraft will differ but, that the basic strategy for avoiding BVI noise will be the same. This explanation is supported by the flight test results given in references 3 and 4.

Figure 3 is a notional chart copied from the HAI Fly Neighborly Guide (ref. 2). This chart indicates two generic flight strategies that are acceptable to pilots and that avoid the flight conditions that are associated with BVI noise. Both strategies decrease the forward speed from the cruise speed to the landing speed and then flare and land. The first strategy is to use a low rate of descent until the speed is decreased to about 60 kt and then increase the rate of descent. The second strategy is to increase the rate of descent while still at high speed. These strategies are generic because the conditions that cause BVI differ for each rotorcraft. But, these strategies indicate speeds and rates of descent that are acceptable to pilots.

The goal of the optimization routine is to select from all pilot-acceptable flight paths the one that has the least noise for a given rotorcraft. Figure 4 shows how the notional HAI Fly Neighborly chart can be discretized into a set of 11 possible approach strategies. The MOGA will select one of these 11 strategies, plus one initial altitude and one initial speed. The MOGA will also select a percentage of speed reduction along each of the next 11 segments of the approach. These 14 pieces of information (1 strategy, 1 initial altitude, 1 initial speed, and 11 speed reduction percentages) uniquely describe an acceptable approach path. The best approach path depends not only on the values of the 14 design variables but also on the set of noise hemispheres that describe the noise that is generated by the rotorcraft.
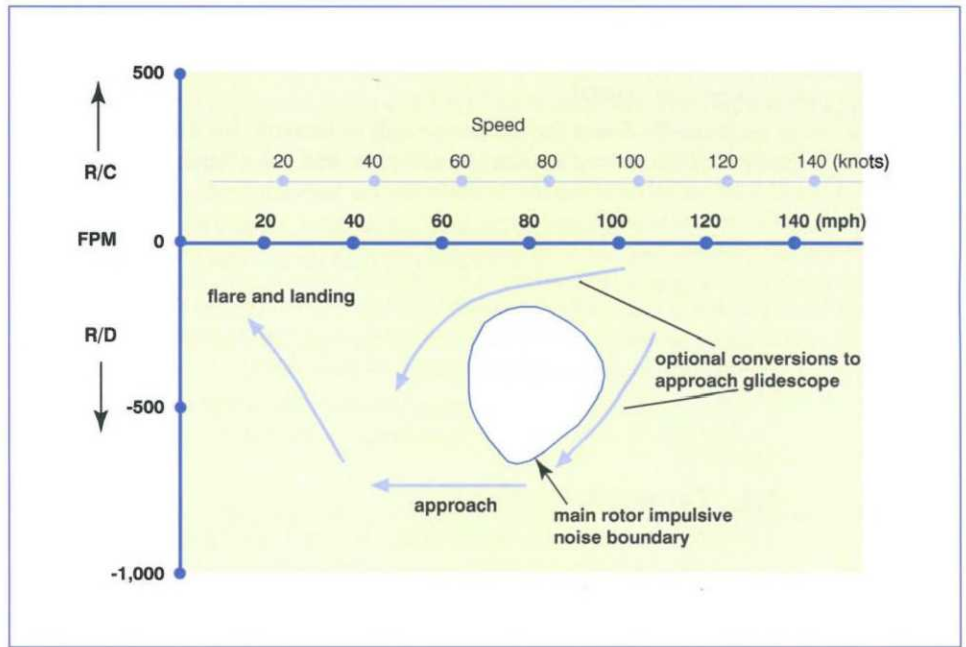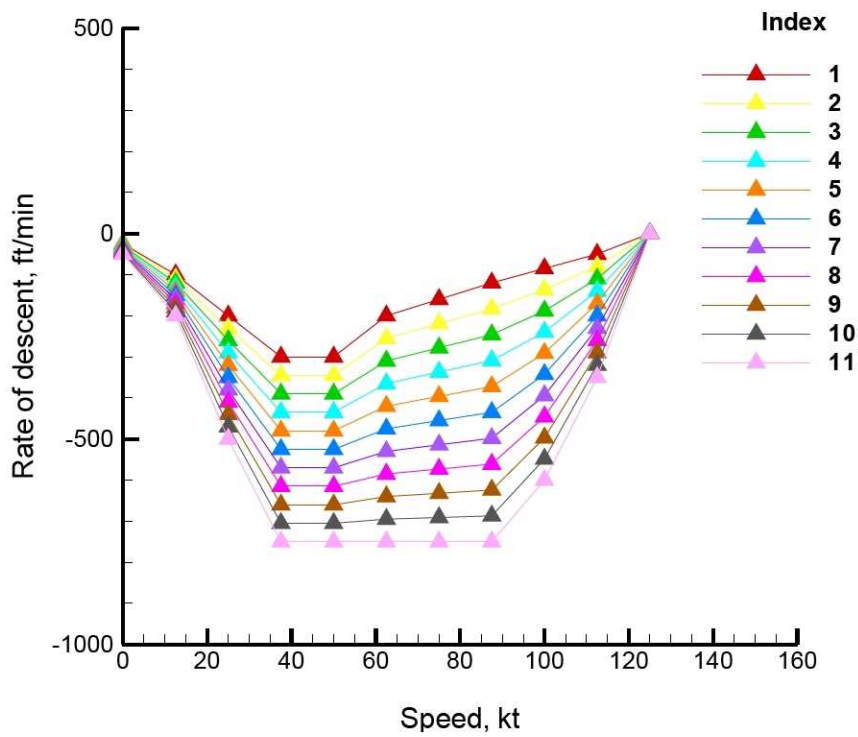
Figure 3. HAI Fly Neighborly chart.

Figure 4. Discrete glide slope options available to MOGA.

Formulation of the Optimization Problem

The candidate approach paths are completely defined by the 14 integer design variables k_j. The first 11 design variables determine the speed and altitude at the end of the first 11 flight path segments, and k_{12} determines the index of the discrete glide slope that is shown in figure 4. Finally, k_{13} and k_{14} determine the initial speed and altitude:

$$s_j = s_{j-1}(1.0 - 0.02k_j) \qquad 1 \le k_j \le 9, \ \ j = 1, ..., 11 \qquad (3)$$

$$s_0 = 145 - 10k_{13} \qquad\qquad 1 \le k_{13} \le 4$$

$$y_0 = 100k_{14} \qquad\qquad\quad 10 \le k_{14} \le 15$$

where y_0 is the initial altitude and s_0 is the initial speed. For any flight-path segment, the reduced speed s_j is determined from the speed in the previous segment by using equation (3). For example, if k_j equals 2, then the new speed is 96 percent of the previous speed. Given speed s_j and index k_{12}, the appropriate rate of descent r_d can be estimated from figure 4. Given r_d and altitude y_{j-1}, the next altitude y_j can be calculated. The calculated values of speed and altitude are used until the terminal conditions of 63 kt and 300 ft are reached. This procedure creates smoothly varying descent flight segments with monotonically decreasing speed and altitude.

The optimization problem can be stated as

> Choose $\quad k_j$
>
> Minimize $\quad R_{ave} + S_{ave}$
>
> Subject to $\quad R_{max} < 2.0$ $\hfill (4)$

where S_{ave} is the average change in SELA and R_{ave} and R_{max} are the average and maximum R over all time steps.

Results: CH−146

Data Available

References 5 and 6 describe the data collection and data reduction processes that are used to create noise hemispheres for the RNM. Reference 6 indicates good agreement between the RNM SELA calculations and the measured SEL noise footprints whenever a sufficient number of high-quality measured noise hemispheres are available. One of the most complete data sets is for the CH−146 Griffon. (Note: This is the Canadian designation for the Bell 412SP.) Figure 5 shows the speed and the rate of descent for the 26 hemispheres used to test the optimization strategy. Color contour plots of each of the 26 hemispheres were inspected and informally rated for their ability to cause high community noise. The shape and color of the symbols in figure 5 indicate flight conditions that will cause the highest and lowest noise levels.
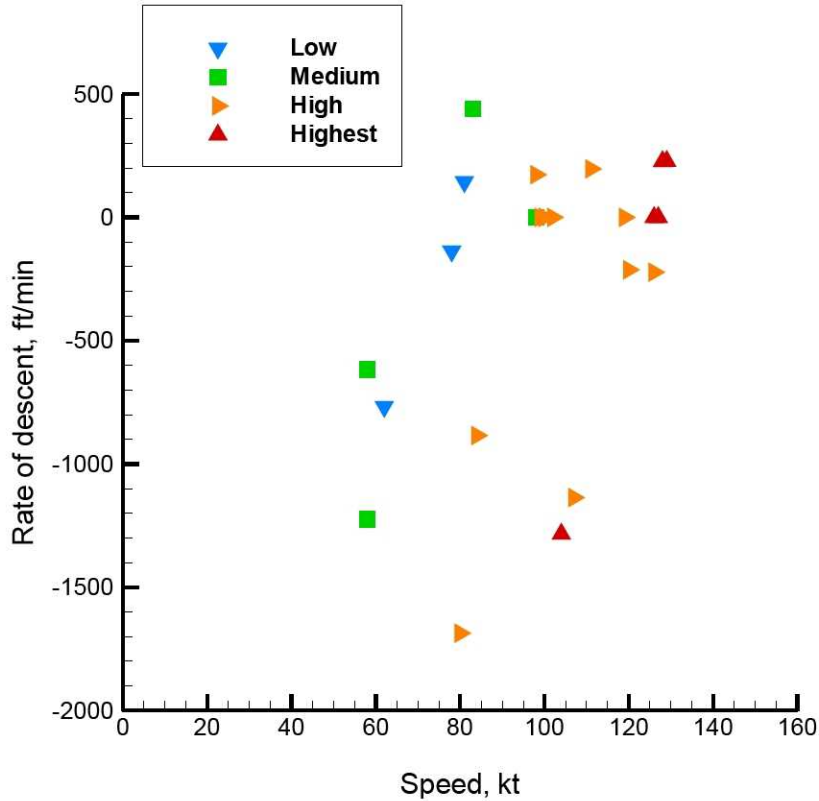
Figure 5. Rate of descent and speed for CH–146 data (symbol color and shape indicate relative noise levels).

Sample Results

With the application of the optimization strategy described earlier, the MOGA successfully identified a flight path that reduced the SELA under the flight track. Figures 6 and 7 compare the SELA noise footprints that are produced by the standard 6-deg approach and the optimized approach. The color scale for these noise footprints was chosen to allow a comparison between the CH–146 results and the MD–900 results. The black dots on figures 6 and 7 indicate noise assessment locations. The SELA is reduced by 1 to 4 dB in most parts of the footprint. This amount of reduction is significant, although not as dramatic as was anticipated; it is consistent with earlier low-noise operations studied by Yoshikami and Cox (ref. 3).
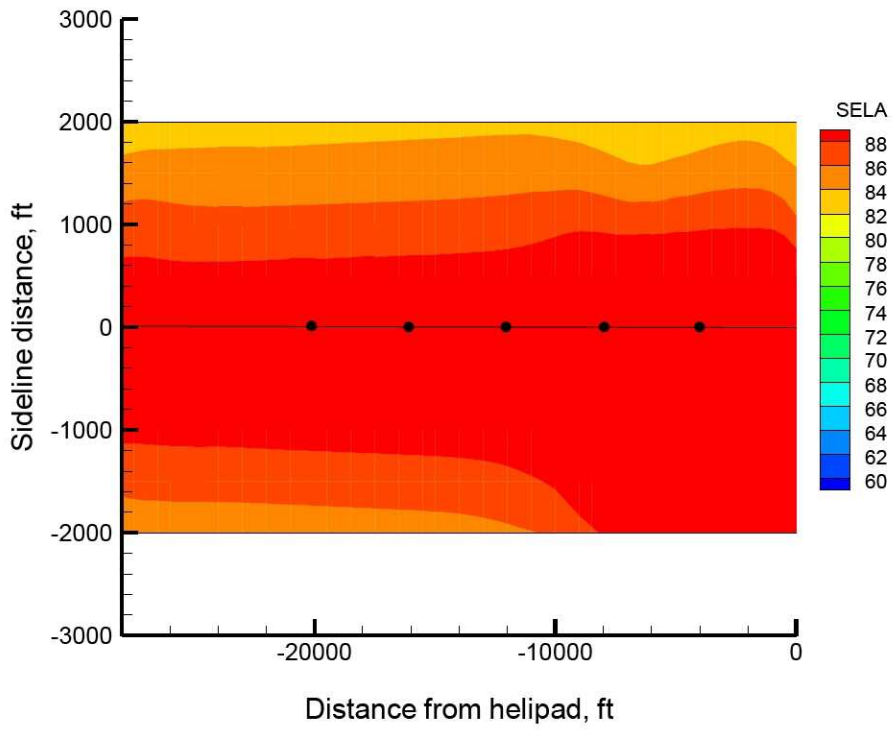
Figure 6. Noise footprint for CH̃146 on a standard approach.
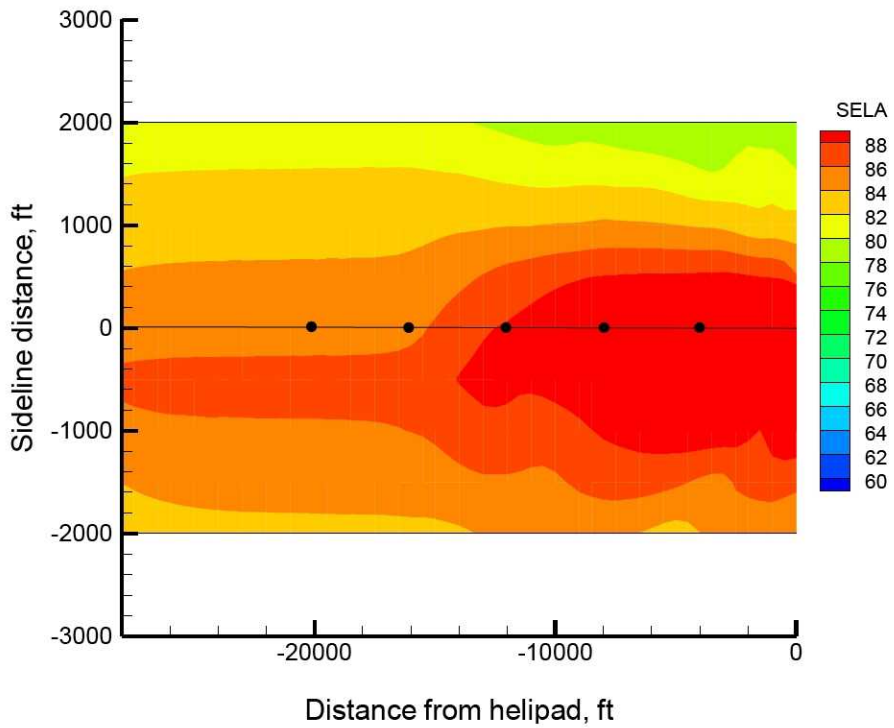
Figure 7. Noise footprint for CH̃146 on the optimized approach.
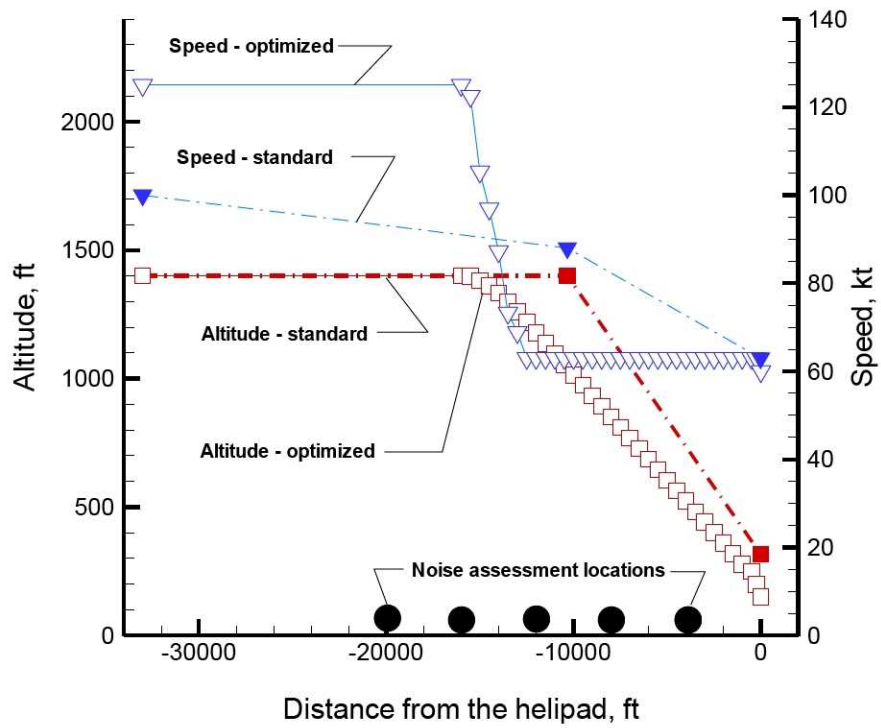
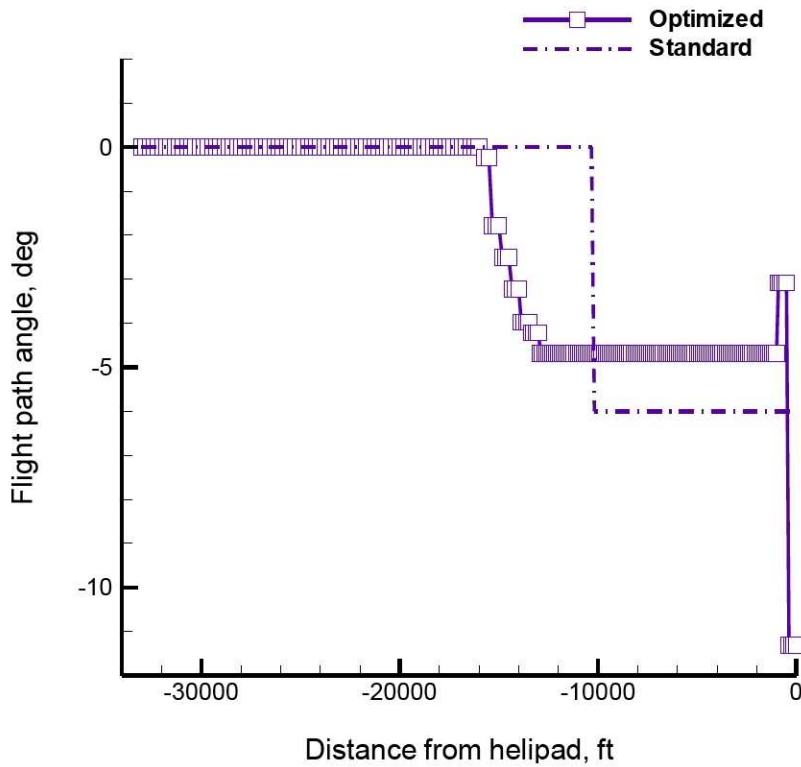**Figure 8. Altitude and speed as a function of distance for CH−146 approach paths.**

Figure 9. Flight path angle as a function of distance.
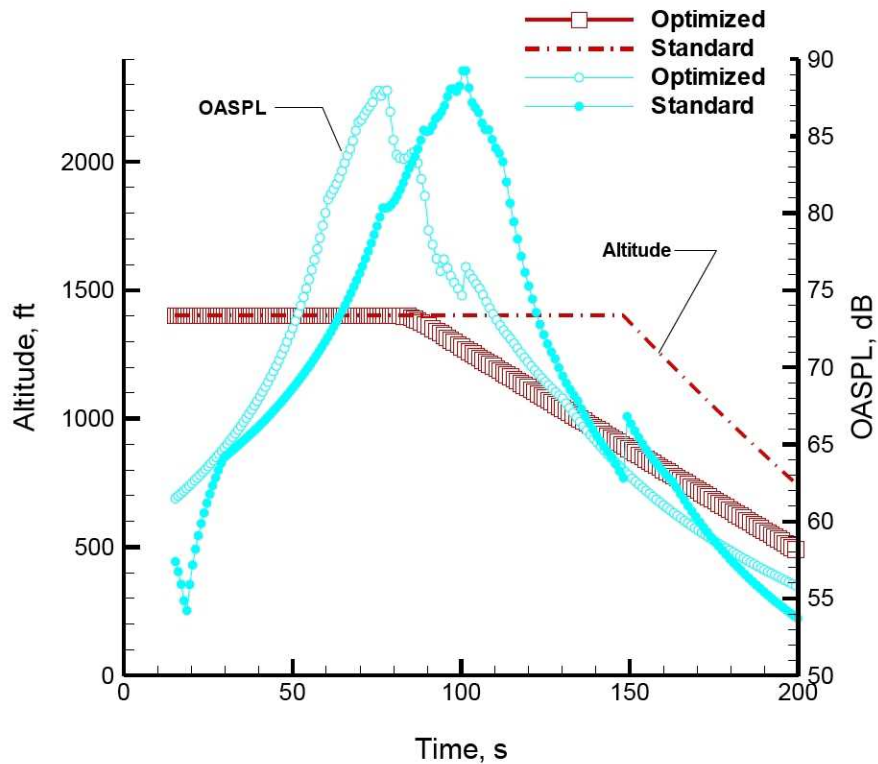
Optimized Approach Path

Figure 8 compares the standard and optimized approach paths. The standard path is a 6-deg approach that starts at an altitude of 1400 ft and at a speed of 100 kt (see solid symbols in fig. 8). The optimized path starts at an altitude of 1400 ft and has a higher speed during the level-flight segment (see the open symbols in fig. 8). Both paths are supposed to end at the same speed and altitude (i.e., 63 kt at 300 ft); however, the optimized path includes a few extra segments below 300 ft, as shown in figure 8. These extra segments are excluded from the calculation of R_{max} and R_{ave}, but may have a slight effect on the value of S_{ave}.

Figures 8 and 9 show that the optimized path begins to descend sooner and more gradually as compared with the path of the 6-deg approach. Intuitively, this result makes sense because a shallow flight path angle typically avoids the maximum BVI operating conditions, while the higher speed allows the rotorcraft to pass the noise assessment locations more quickly. Passing a location quickly is advantageous because it affects the duration correction in the SELA evaluation. This optimization result is consistent with the experimental evidence that is given in references 3 and 4.

Analysis of Results

The test of the optimization strategy using the CH–146 data set was successful. That is, a flight path was identified that had reduced noise and that met the criteria for pilot acceptance. During this initial study, a number of areas were identified where improvements could be made to the RNM code and to the optimization strategy.

First, understanding why the optimized flight path is an improvement over the standard 6-deg approach is necessary. Figures 8 through 10 clearly show that the optimized approach allowed for passing most of the noise assessment locations with a higher speed but at a lower flight path angle than for the standard approach. And, figure 10 clearly shows that, at a given noise measurement location along the flight track, the optimized approach produced lower maximum sound levels and reduced the amount of time that the sound was near the maximum level. Figure 10 plots altitude versus time rather that altitude versus distance. Notice that the altitude was generally lower for the optimized approach path than for the standard 6-deg approach path. Increasing the distance from the vehicle to the noise-measuring location is important, but optimizing the rate of descent and the speed at each time step appears to be the most effective way to reduce sound levels on the ground.

Figure 10. Altitude and OASPL as a function of time at a selected location.

Examination of the convergence behavior of the optimization process revealed that many seemingly good approach paths were rejected as infeasible. Diagnosis of this behavior suggests that the constraint $R_{max} < 2$ was too restrictive if we consider that all candidate approach paths began their descent at a fixed distance (i.e., 16,000 ft) from the helipad. The only way to meet the R_{max} constraint was to have a high initial altitude or to begin the descent further than 16,000 feet from the helipad. Therefore, the optimization procedure was modified to allow the descent start distance to vary. This modification was tested with the MD−900 data set.

Another issue of concern was the reliability of the measured flight test data. Each of the CH−146 noise hemispheres was created from a limited amount of flight test data. During these flight tests, the pilot tried to maintain a constant speed and a constant flight path angle while flying over an array of microphones. Reference 4 reports that the mean altitude errors in the 1995 acoustic test flights were smaller than the ±30 ft window that was specified for noise certification. However, the rate-of-descent tracking performance was less than desirable (e.g., ±250 ft/min in run number 14). In other words, to stay on the specified glide slope, the pilots were constantly making small adjustments to speed and flight path angle, which resulted in accelerations and decelerations throughout the measurement process. Chen et al. (ref. 4) explain how these factors increase the uncertainty in the measured acoustic data. The CH−146 data set is expected to contain similar levels of uncertainty. More recent acoustic test flights have reduced the measurement uncertainties significantly with improvements in testing procedures, piloting techniques, and pilot aids such as "heads-up displays" (e.g., see ref. 9).

In addition to the above issues, the interpolation methods in the RNM code also need to be improved. At any given time step on a flight path, the code uses the provided noise hemispheres to predict the OASPL at a given set of locations. However, the flight condition at that time step typically does not exactly match

13

any noise hemisphere in the data set. To perform this calculation, the RNM internally chooses up to four hemispheres that are at flight conditions that closely approximate the current flight condition and interpolates between these hemispheres. If no flight conditions are close enough, then no interpolation is performed, and the hemisphere at the closest flight condition is chosen. Unless the noise hemisphere database contains an adequate set of flight conditions, this simple interpolation procedure can create discontinuties in the predicted OASPL time history (see fig. 11). The abrupt jump that can be seen in figure 11 (near the point at which time equals 55 s) is caused by switching from one hemisphere to the next in a discontinuous manner. When the RNM uses a scheme that forces interpolation between (up to four) noise hemispheres, the jump in the OASPL is eliminated. This can be accomplished by modifying the RNM parameters that determine when a flight condition is close enough to allow interpolation between hemispheres. For general cases, even the modified interpolation scheme produces questionable results unless the noise hemisphere data set contains a large array of closely spaced flight conditions. Unfortunately, this large array of flight conditions is difficult to obtain because of the high cost of flight testing and the requirement for highly reliable measurements.

To minimize the above effects, the optimization procedure was modified. For each approach path that was generated by MOGA, two RNM predictions such as the two in figure 11 were made. If the two predictions differed dramatically, then the MOGA penalized this candidate path by adding another term in the objective function (eq. 4). With this modification, all candidate paths with questionable noise estimates were avoided, and the results shown in figures 6 through 10 were produced. However, a large number of attractive candidate paths have been avoided as a result of this interpolation issue.
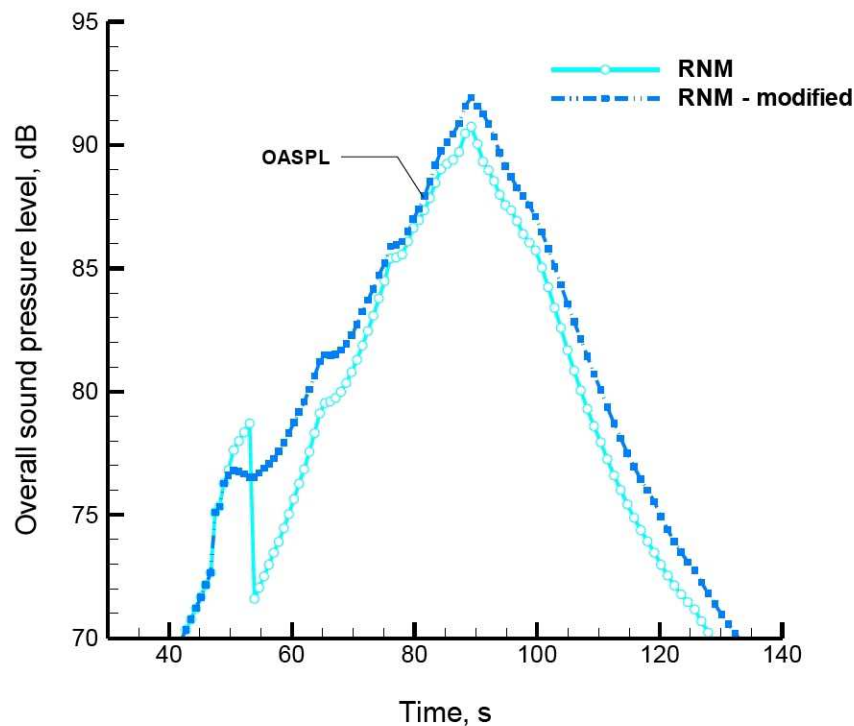

Figure 11. Effect of interpolation parameters on RNM noise prediction.

Results: MD−900

Data Available

The second test of the optimization procedure used noise hemispheres at 36 flight conditions for the MD−900 rotorcraft. These noise hemispheres were generated with the Comprehensive Analytical Model of Rotorcraft Aerodynamics and Dynamics II (CAMRAD-II) and the Ffowcs Williams Hawkings solver, PSU-WOPWOP, as discussed in reference 11. Given a model of the rotorcraft, CAMRAD-II determines the trim state (i.e., aerodynamics, blade motion, vehicle attitude, etc.) that is required to fly along a specified quasi-steady flight path. The aerodynamics and the blade motion of the vehicle are used in PSU-WOPWOP to compute the acoustic pressure time histories at a set of observers (i.e., microphone locations). These acoustic pressure time histories are analyzed to compute the discrete frequency noise content at each location. These frequency data are then converted to one-third octave band frequency data. The observers for all of these cases were on a hemisphere below the vehicle at a distance of 10 rotor radii. This procedure was repeated for all 36 flight conditions to generate a noise hemisphere database to be used with the RNM.

These 36 flight conditions (see fig. 12) were chosen for this study to provide improved coverage of the flight speeds and descent rates of interest. This strategy provided the RNM with enough data to avoid rejection of any flight path by the optimization scheme based on the interpolation penalty that was discussed in the previous section.
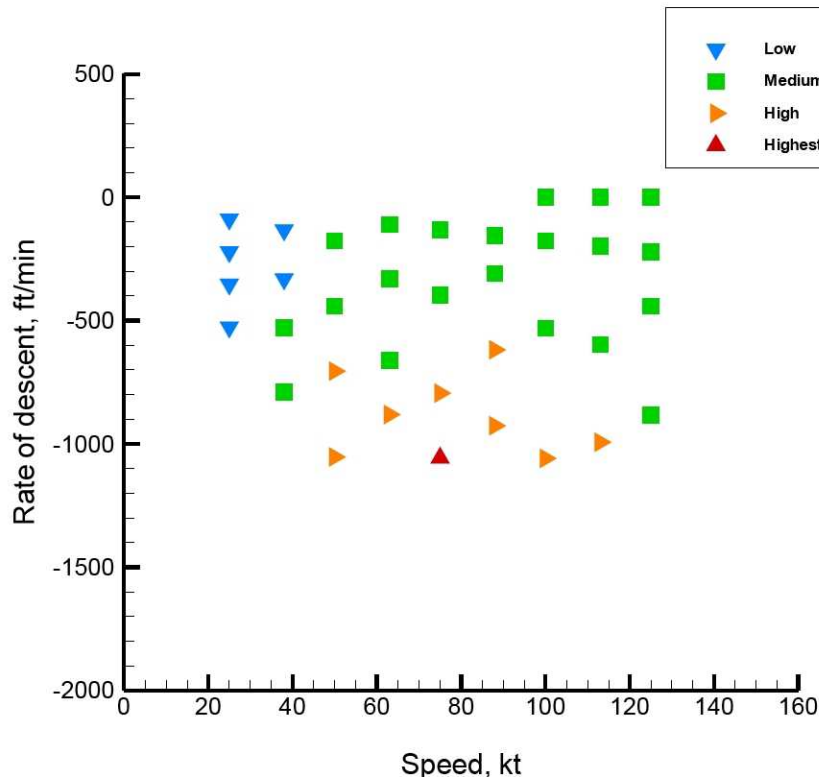

Figure 12. Rate of descent and speed combinations of predicted MD−900 data set.

With the previous flight-path restrictions removed, the MD–900 optimization strategy had a larger number of feasible flight paths from which to choose. For example, figures 13 and 14 show a wide variety of acceptable low-noise flight paths that were generated by the MOGA (i.e., $R_{max} < 2$ and $S_{ave} < 0$ for each path). Figure 13 shows altitude versus distance to the helipad; figure 14 shows the corresponding speed versus distance. These plots show only the descending portion of the approach. Each approach started at the selected initial altitude y_0 and the initial speed s_0 and at a distance of 35,000 ft from the helipad. Each flight path was level and maintained a constant speed until the descent portion of the path was reached.
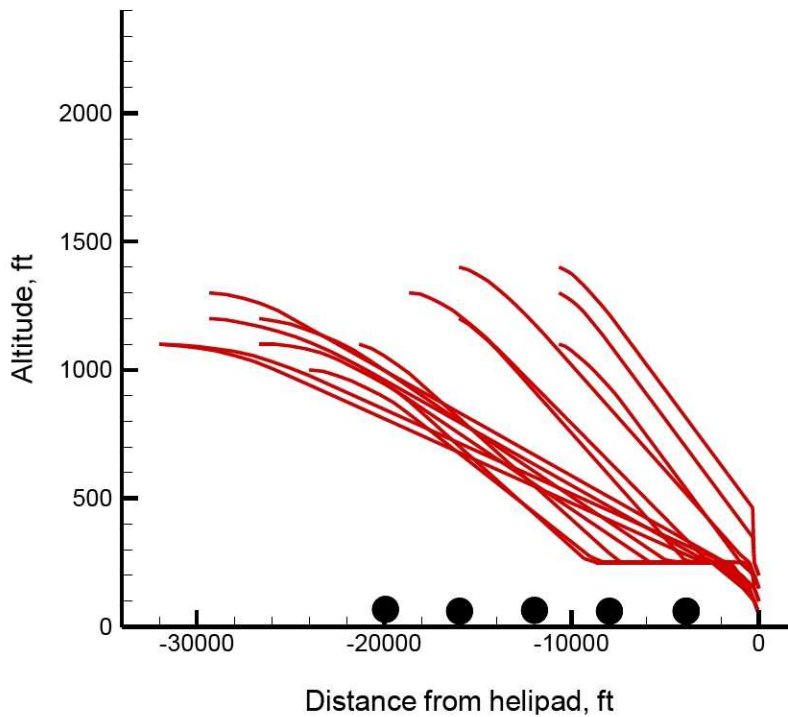
**Figure 13. Possible approach paths for MD–900 helicopter.**

16
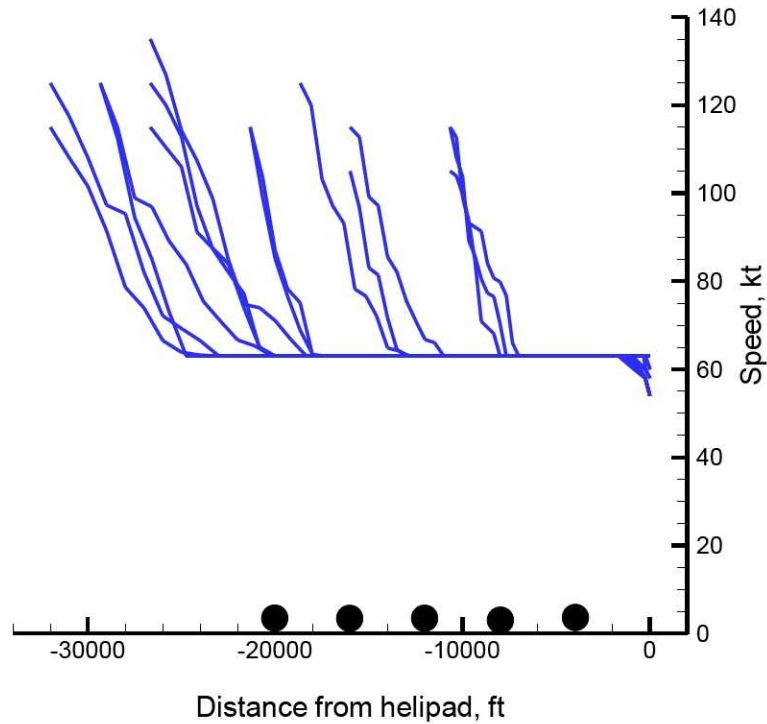
**Figure 14. Possible speed schedules for MD−900 helicopter.**

Sample Results

Three sets of optimization results are presented. First, the optimization problem that was stated in equation (4) was repeated for the MD−900 rotorcraft. Recall that the constraint $R_{max} < 2.0$ was selected because it matched the standard 6-deg approach case. Next, the optimization problem was repeated with the constraint set to $R_{max} < 1.2$. This constraint was selected to produce a flight path that was more acceptable to passengers. Finally, the same problem ($R_{max} < 1.2$) was repeated with a larger number of candidate flight paths. Figure 15 compares the noise footprints for the standard 6-deg approach with those optimized approaches. Figure 16 compares the speed and altitude for the three approaches. Clearly, both optimized approaches reduce community noise. Figure 17 shows how the first two optimized approaches compare with the glide slopes that were recommended by the HAI Fly Neighborly document (fig. 3).
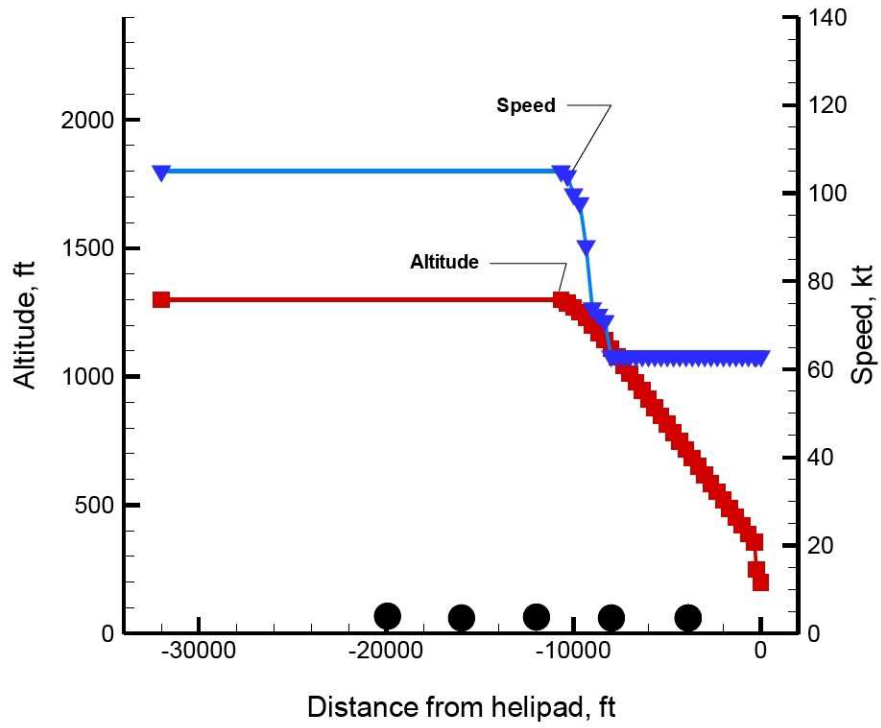
17

(a) Standard approach.

(b) $R_{max} < 2.0$ using 300 RNM runs.
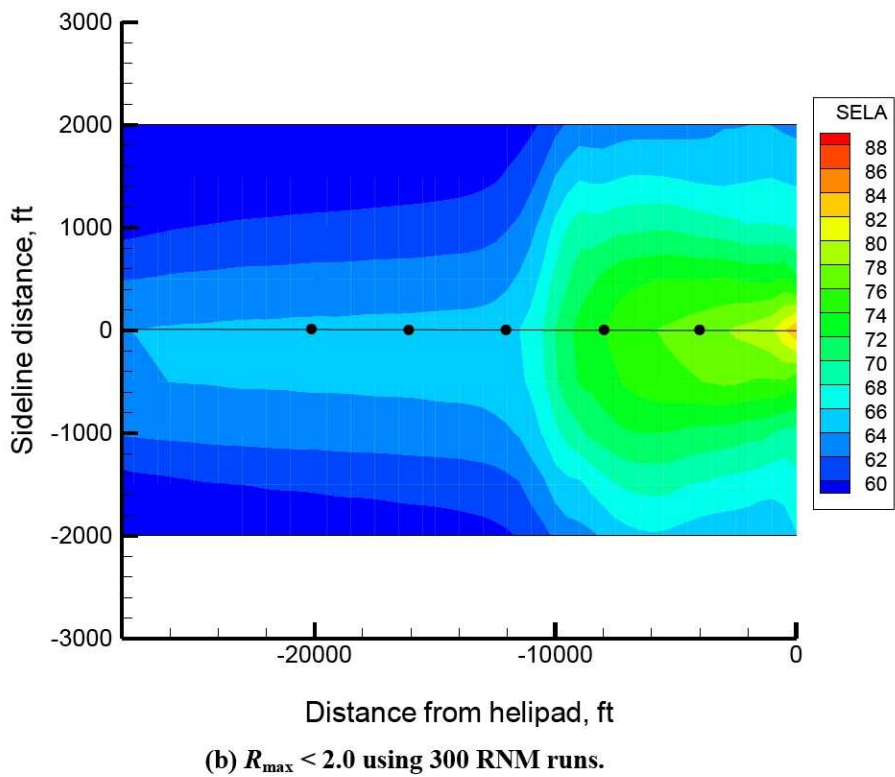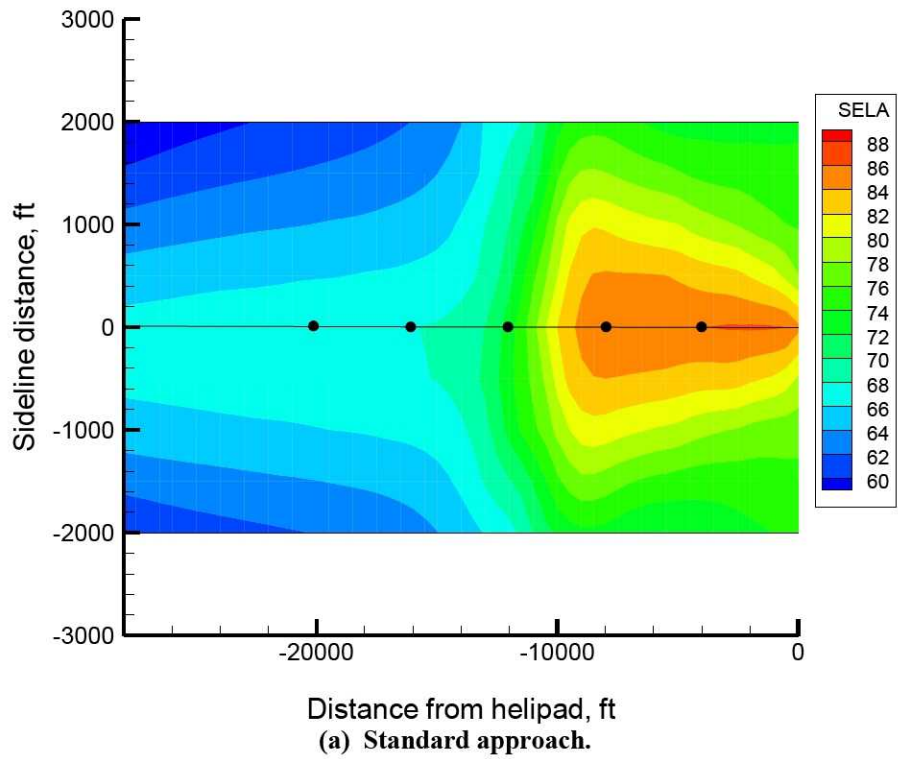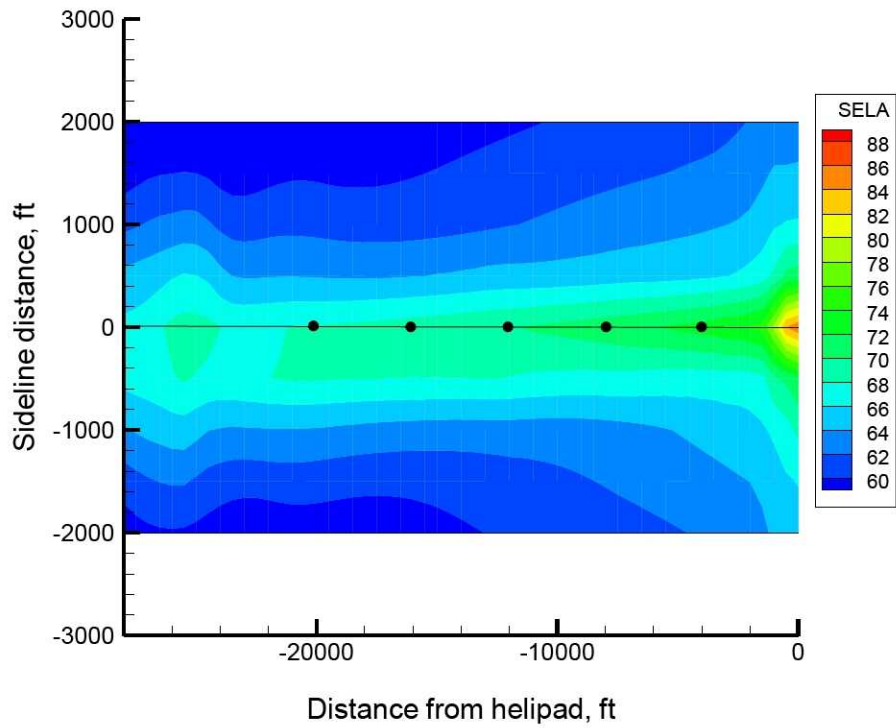
(c) $R_{max} < 1.2$ **using 300 RNM runs.**
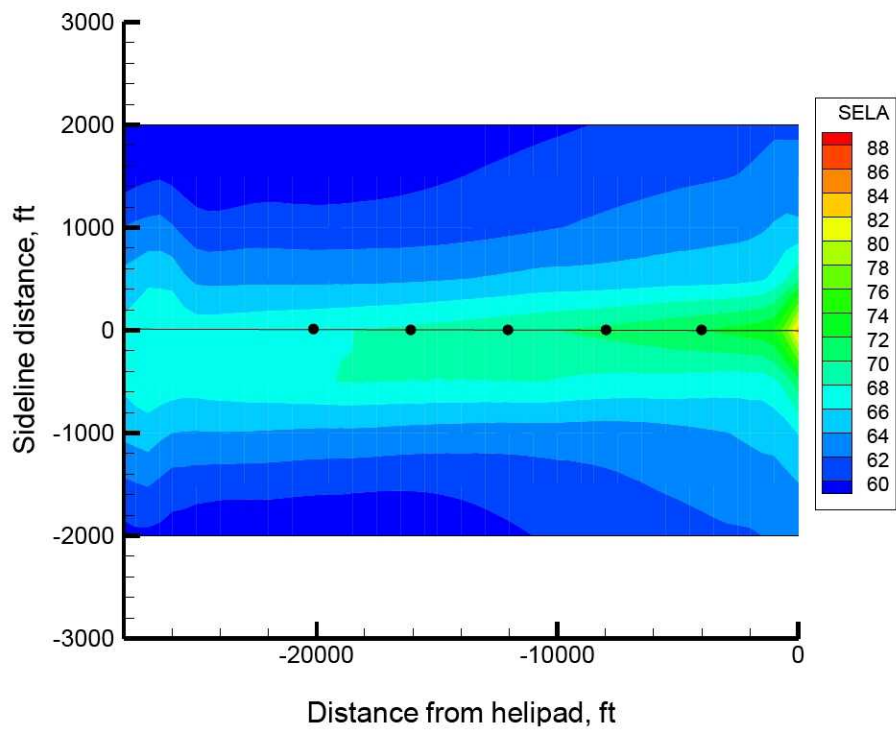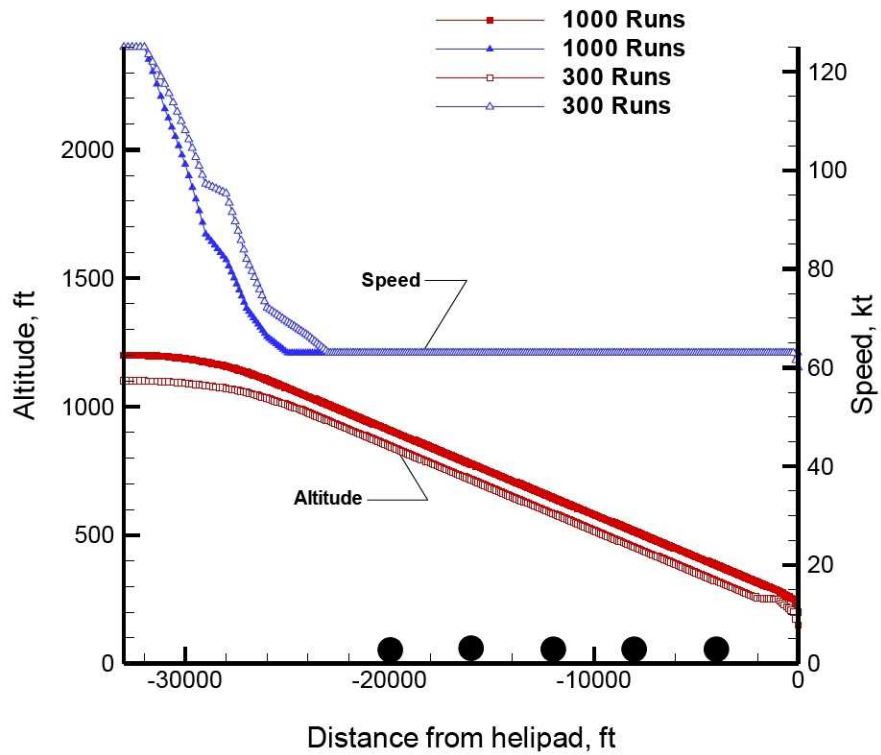

(d) $R_{max} < 1.2$ **using 1000 RNM runs.**
Figure 15. Noise footprints for MD-900 on standard and optimized approaches.

19

(a) $R_{max} < 2.0$

(b) $R_{max} < 1.2$

Figure 16. Speed and altitude as a function of distance for optimized approach paths.
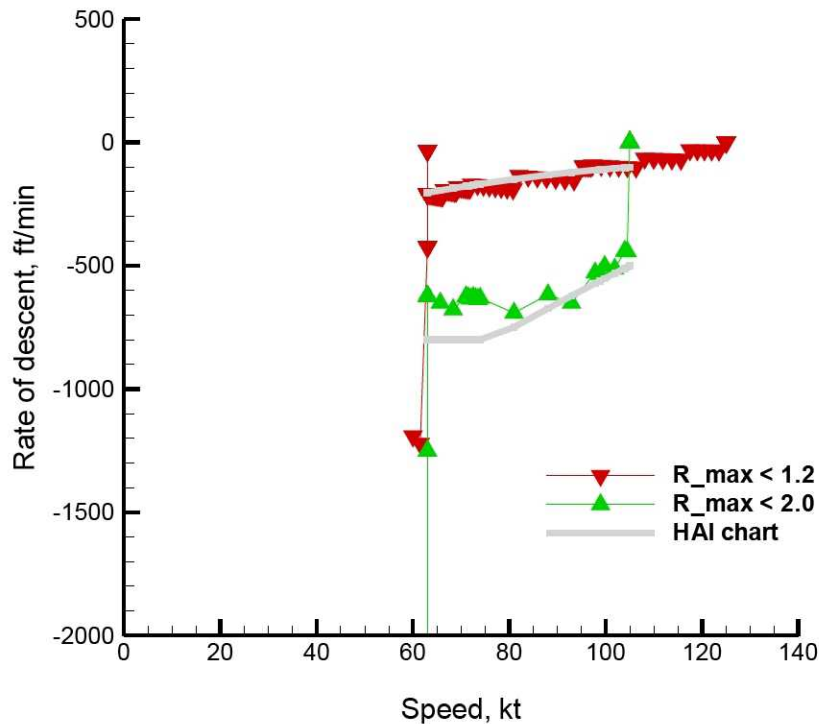
Figure 17. Optimized glide slopes compared to HAI recommendations.

Analysis of Results

The noise footprints in figures 6 and 15 demonstrate definitively that the five-bladed MD−900, which has a maximum gross takeoff weight (GTW) of 6,500 lb, generates less noise than the four-bladed 12,000 lb GTW CH−146. This can be partly explained by the fact that the measured CH−146 data contains contributions from all noise sources, while the predicted MD−900 data contains rotor blade noise only. But, these are also very different vehicles. The MD−900 is a smaller vehicle that has no tail rotor (NOTAR) and was designed for reduced noise. Thus, these two data sets provide a good test of the approach trajectory optimization procedure.

Fortunately, the optimization procedure can be successful whether or not the MD−900 noise hemispheres are underpredicted. As long as the trends are correct, the absolute levels that are produced by the candidate approaches are inconsequential because the MOGA algorithm is not a gradient-based method. As long as the RNM correctly identifies which of two candidate approaches generates less noise, the MOGA will function as expected. Based on comparisons between the MD−900 predicted data and a limited amount of measured data, the authors believe that the trends are representative of this class of vehicle.

For the optimization strategy to be considered successful, we must be able to demonstrate that the best approach path has been found. One way to demonstrate this is to make additional runs with the MOGA. The original results were found by using only 300 RNM predictions. If the MOGA is allowed to run the RNM 1000 times, then a similar but improved approach path can be found (see figure 16b). The improved approach path that was identified with 1000 RNM runs is smoother and reduces S_{ave} by an additional 0.5 dB.

21

Another way to assess the results is to use a design of experiments (DOE), as suggested in reference 12. One DOE is used to examine other candidate paths that are near the optimized approach path by perturbing one design variable at a time. A second DOE (e.g., Latin hypercube sampling) is used to examine candidate paths from other parts of the design space. These DOE studies found several other good approach paths that were quite similar to the optimized approach paths in figure 16. This is further evidence that the MOGA is operating correctly.

The same DOE assessment can be used to test our hypothesis that reducing the average SELA will also reduce the noise footprint. For example, given a noise footprint of SELA values on a uniform grid, define a new objective called A_{ave}:

$$A_{ave} = \frac{1}{h^2} \int_i \int_j \text{SELA}_{ij} \, di \, dj \qquad (5)$$

where h is the grid cell length in ft. Note that a uniform grid is used for convenience; any sufficiently dense grid likely would give similar results. Equation (5) represents the volume under the SELA noise footprint surface and can be approximated by using multidimensional numerical integration. We define A_{ave} as the volume for any candidate approach path, and $A*_{ave}$ as the volume for the optimum approach path found with 1000 RNM runs.

Figures 18 and 19 reveal the correlation between S_{ave} and A_{ave} for a Latin hypercube DOE centered on the optimum design. The optimum design has $R_{max} < 1.2$ and $S_{ave} < -3.2$ dB, indicated by a black diamond in each graph. First, notice in figure 18 that no acceptable design has a lower S_{ave} than the optimum design. Next, notice in figure 19 that a high correlation exists between S_{ave} and A_{ave}. The correlation between these two noise metrics suggests that the MOGA would converge to a similar optimized approach path if A_{ave} were used in the objective function instead of S_{ave}. This hypothesis has not been tested because of the computational expense of calculating 1000 noise footprints.
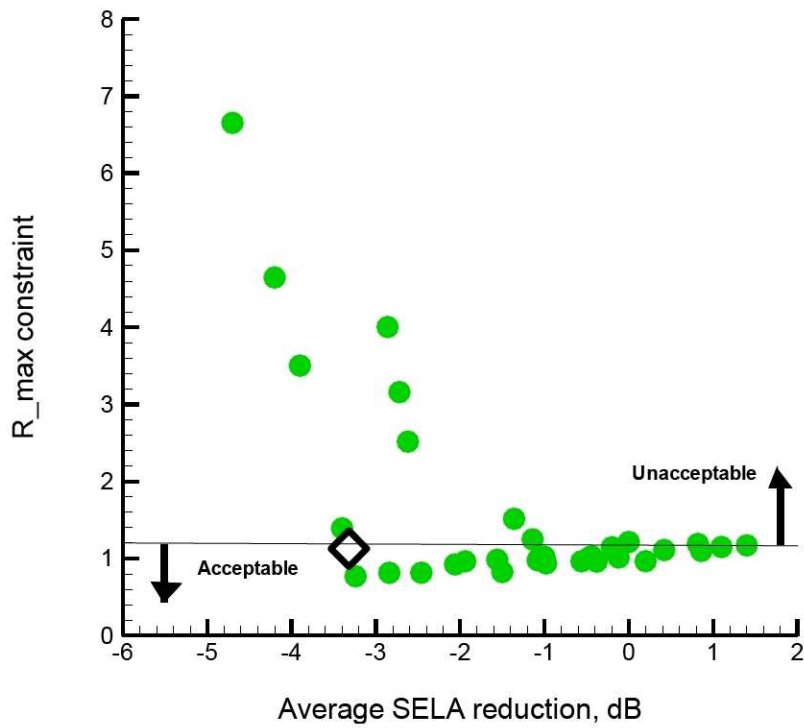
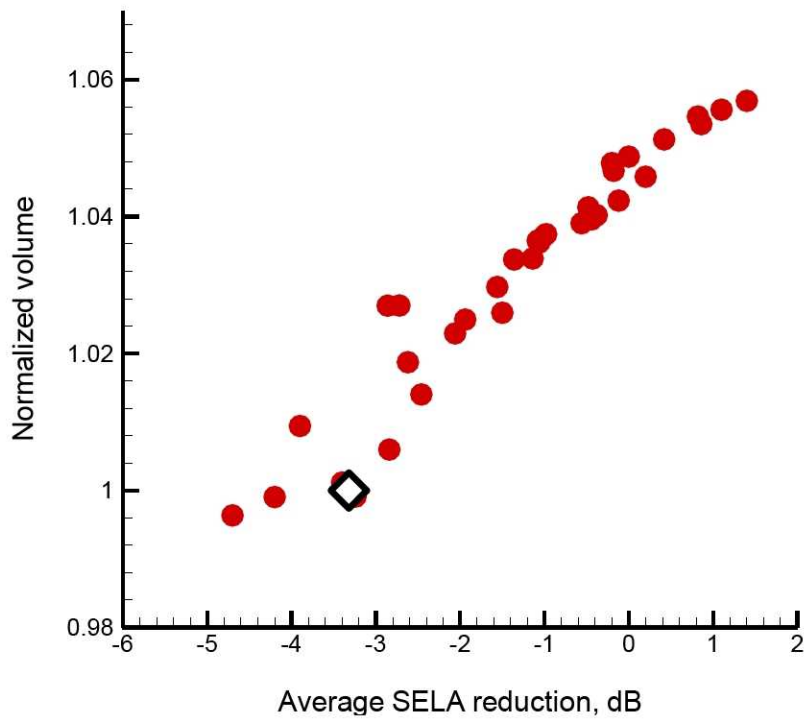**Figure 18. Plot of S_{ave} versus R_{max} for designs near the optimum.**

Figure 19. Plot of S_{ave} versus A_{ave} / A^*_{ave} for designs near the optimum.

Concluding Remarks

Successful Optimization Procedure

Application of the MOGA procedure to two rotorcraft vehicles and their associated acoustic data sets demonstrates the capability of the optimization-based procedure to design quiet approach trajectories. The multi-objective optimization is able to reduce noise at several locations and design an approach path that is likely to be acceptable to the pilot and passengers. The optimized approaches compare favorably with HAI Fly Neighborly recommendations and are consistent with previous low-noise flight test results.

The optimization results are validated by repeating the MOGA procedure with 300 and then 1000 objective function evaluations. The resulting optimized approach paths are quite similar. The results are also validated by using a Latin hypercube DOE to generate alternate approach paths. This DOE study indicates that the MOGA functions correctly. The DOE study further suggests that by intentionally reducing noise at five individual locations the MOGA is also reducing total noise in the area represented by the noise footprint.

Recommended Improvements for Prediction and Optimization

The present research effort points to the need for additional high-quality measured data. The CH–146 data set is the largest set available, yet it does not contain enough information to meet the needs of the MOGA optimization procedure. Without a set of noise hemispheres that completely and adequately covers all of the approach angles and speeds of interest, the current RNM interpolation scheme introduces errors that impact the optimization procedure.

On the other hand, flight testing is expensive, and some approach paths are difficult or even dangerous to fly. One attractive possibility is to acquire a limited set of high-quality measurements, including characterization of the measurement uncertainty. Once high-quality data are available, the dense set of hemispheres that is required by the RNM can be created as a preprocessing step by careful interpolation between measured hemispheres. DOE and optimization procedures such as the ones discussed in this paper can be used to assess the value of this preprocessing step.

To improve the prediction of safe, low-noise optimized flight paths, a set of measured or predicted hemispheres that adequately cover the range of angles and flight speeds should be acquired for any rotorcraft of interest. The following recommendations are made to improve the functionality and useability of the current RNM: (1) the RNM should output warnings if the requested flight conditions are outside the range of flight conditions in the noise hemisphere data, (2) inputs to the RNM should be adjusted so that safe and comfortable flight paths are easy to specify, and (3) RNM calculations should include some indication or estimate of the uncertainty in the predicted noise levels. These recommendations have been implemented in a modified version of the RNM and in the modified optimization procedure that is described in this paper and have been tested with the CH–146 data set. The results show optimized flight paths that meet our criteria for pilot acceptability and that have reduced noise in comparison with the standard approach.

The successful MD–900 helicopter optimization results suggest a need to rethink the manner in which flight test matrices are determined and the manner in which noise hemispheres are processed. The results show that, when the MOGA procedure uses a data set that adequately covers the range of speeds and rates of descent of interest, the optimization converges to a quiet approach trajectory. These results also suggest the need to rethink and improve the interpolation algorithms that are used by the RNM. The quality of the optimized approach path can be improved by allowing an increased number of RNM function

evaluations. However, even with 300 function evaluations, the optimized path is shown to be an excellent flight path that meets the given criteria and constraints for the MD−900 helicopter.

References

1. Orr, S. and Narducci, R.: "Framework for Multidisciplinary Analysis, Design, and Optimization with High Fidelity Analysis Tools," NASA CR−2009−215563, February 2009.

2. Helicopter Association International: *Fly Neighborly Guide,* Second Edition, *1993*. URL: http://www.rotor.com/ (accessed May 21, 2009).

3. Yoshikami, S. A. and Cox, C. R.: "FAA/HAI Helicopter Flight Operations Noise Tests and Initial Results," Presented at American Helicopter Society 41st Annual Forum, Fort Worth, TX, May 15−17, 1985.

4. Chen, R. N.; Hindson, W. S.; and Mueller, A. W.: "Acoustic Flight Tests of Rotorcraft Noise-Abatement Approaches Using Local Differential GPS Guidance," NASA TM-110370, September 1995.

5. Conner, D. A.; Burley, C. L.; and Smith, C. D.: "Flight Acoustic Testing and Data Acquisition for the Rotor Noise Model (RNM)," Presented at American Helicopter Society 62nd Annual Forum, Phoenix, AZ, May 9-11, 2006.

6. Conner, D. A. and Page, J. A.: "A Tool for Low Noise Procedures Design and Community Noise Impact Assessment: The Rotorcraft Noise Model (RNM)," Presented at Heli Japan 2002, Tochigi, Japan, November 11−13, 2002.

7. Deb, K.; Pratap, A.; Agarwal, S.; and Meyarivan, T.: "A Fast and Elitist Multiobjective Genetic Algorithm: NSGA-II," *IEEE Transactions on Evolutionary Computation*, Vol. 6, No. 2, April 2002.

8. Conner, D. A.; Marcolini, M. A.; Decker, W. A.; Cline, J. H.; and Edwards, B. D.: "XV-15 Tiltrotor Low Noise Approach Operations," Presented at the American Helicopter Society 55th Annual Forum, Montreal, Quebec, Canada, May 25−27, 1999.

9. Decker, W. A.: "Handling Qualities Evaluation of XV-15 Noise Abatement Landing Approaches Using a Flight Simulator," Presented at the American Helicopter Society 57th Annual Forum, Washington, DC, May 9−11, 2001.

10. Bennett, R. L. and Pearsons, K. S.: "Handbook of Aircraft Noise Metrics," NASA-CR-3406, March 1981.

11. Boyd, D. D.; Burley, C. L.; and Conner, D. A.: "Acoustic Predictions of Manned and Unmanned Rotorcraft Using the Comprehensive Analytical Rotorcraft Model for Acoustics (CARMA) Code System," Presented at the American Helicopter Society International Specialists' Meeting on Unmanned Rotorcraft, Phoenix, Arizona, Jan. 18−20, 2005.

12. Santner, T. J.; Williams, B. J.; and Notz, W. I.: *The Design and Analysis of Computer Experiments,* Springer-Verlag, New York, NY, 2003.

REPORT DOCUMENTATION PAGE					Form Approved OMB No. 0704-0188

The public reporting burden for this collection of information is estimated to average 1 hour per response, including the time for reviewing instructions, searching existing data sources, gathering and maintaining the data needed, and completing and reviewing the collection of information. Send comments regarding this burden estimate or any other aspect of this collection of information, including suggestions for reducing this burden, to Department of Defense, Washington Headquarters Services, Directorate for Information Operations and Reports (0704-0188), 1215 Jefferson Davis Highway, Suite 1204, Arlington, VA 22202-4302. Respondents should be aware that notwithstanding any other provision of law, no person shall be subject to any penalty for failing to comply with a collection of information if it does not display a currently valid OMB control number.
PLEASE DO NOT RETURN YOUR FORM TO THE ABOVE ADDRESS.

1. REPORT DATE (DD-MM-YYYY) 01- 06 - 2009	2. REPORT TYPE Technical Memorandum	3. DATES COVERED (From - To)

4. TITLE AND SUBTITLE Design of Quiet Rotorcraft Approach Trajectories	5a. CONTRACT NUMBER
	5b. GRANT NUMBER
	5c. PROGRAM ELEMENT NUMBER
6. AUTHOR(S) Padula, Sharon L.; Burley, Casey L.; Boyd, David D., Jr.; Marcolini, Michael A.	5d. PROJECT NUMBER
	5e. TASK NUMBER
	5f. WORK UNIT NUMBER 877868.02.07.07

7. PERFORMING ORGANIZATION NAME(S) AND ADDRESS(ES) NASA Langley Research Center Hampton, VA 23681-2199	8. PERFORMING ORGANIZATION REPORT NUMBER L-19701

9. SPONSORING/MONITORING AGENCY NAME(S) AND ADDRESS(ES) National Aeronautics and Space Administration Washington, DC 20546-0001	10. SPONSOR/MONITOR'S ACRONYM(S) NASA
	11. SPONSOR/MONITOR'S REPORT NUMBER(S) NASA/TM-2009-215771

12. DISTRIBUTION/AVAILABILITY STATEMENT
Unclassified - Unlimited Subject Category 71 Availability: NASA CASI (443) 757-5802

13. SUPPLEMENTARY NOTES

14. ABSTRACT
A optimization procedure for identifying quiet rotorcraft approach trajectories is proposed and demonstrated. The procedure employs a multi-objective genetic algorithm in order to reduce noise and create approach paths that will be acceptable to pilots and passengers. The concept is demonstrated by application to two different helicopters. The optimized paths are compared with one another and to a standard 6-deg approach path. The two demonstration cases validate the optimization procedure but highlight the need for improved noise prediction techniques and for additional rotorcraft acoustic data sets.

15. SUBJECT TERMS
Genetic algorithm; Noise reduction; Rotary wing aircraft; Trajectories

16. SECURITY CLASSIFICATION OF:			17. LIMITATION OF ABSTRACT	18. NUMBER OF PAGES	19a. NAME OF RESPONSIBLE PERSON STI Help Desk (email: help@sti.nasa.gov)
a. REPORT	b. ABSTRACT	c. THIS PAGE			19b. TELEPHONE NUMBER (Include area code)
U	U	U	UU	30	(443) 757-5802

Standard Form 298 (Rev. 8-98)
Prescribed by ANSI Std. Z39.18